A Comparative Study of Acoustic and Elastic Impedance Seismic Models for Rock Property Prediction: An Example from XYZ Field, Nigeria

Difference Odeyovwi Ogagarue*

Department of Earth Sciences, Federal University of Petroleum Resources, Effurun, Nigeria

Email: ogagarue.odeyovwi@fupre.edu.ng

Abstract

A comparative case study of acoustic and elastic impedance seismic inversion for reservoir litho-fluid delineation in XYZ field, Nigeria is presented. The well-studied has four reservoirs. Acoustic impedance inversion carried out on near angle stack was successful in showing the tops of three reservoirs and their lateral extents, but failed to successfully delineate the top of the major reservoir. Fortunately, a shear sonic log was acquired in the well, and a far angle PSTM stack was available for the field. Combining the shear sonic log with the available compressional sonic and density logs, an elastic impedance log was generated at 36^0, corresponding to the incidence angle for the far offset stack, and was used to invert the far angle stack for elastic impedance. The elastic impedance inversion was successful in showing the major reservoir zone as well as clearly delineating its top and lateral extent. It was observed that the acoustic impedance log used for inverting the near angle stack was near constant through the top reservoir transition and this may have accounted for the failure of the acoustic impedance inversion to delineate the top and lateral extent of the reservoir. This paper focuses on comparing the results of the inversions targeted at the main reservoir, highlighting possible reasons for failure and success of the individual inversion method.

Keywords: Acoustic impedance; Elastic impedance; Inversion; Near angle stack; Far angle stack.

----

* Corresponding author.

1. Introduction

The basic objective of seismic inversion is to transform seismic reflection data into a quantitative rock property, descriptive of the reservoir [1]. The ability to estimate acoustic impedance and a parameter related to shear impedance increases the interpreter's ability to discriminate between different lithologies and fluid phases [2], resulting in a detailed reservoir characterization for improved hydrocarbon recovery. This is an improvement over conventional seismic interpretation which relies on the seismic data alone to map geological structures and identify potential exploration targets.

Angle-limited post stack volumes provide a simple way to examine the variations of seismic amplitudes with angle of incidence. The stacks are often generated into near, mid or far volumes corresponding to angles of incidence, such that amplitude variations in these volumes in target zones are mainly indicative of the reservoir fluid. The amplitudes of near angle stacks relate to changes in acoustic impedance [3] which can be well correlated with lithologic changes, and to invert near angle stack for acoustic impedance, acoustic impedance (AI) is derived directly from the compressional sonic and density logs to provide input for the inversion algorithm. This is the conventional post stack inversion method and it has proven successful in many rock property prediction studies [4,5,6,7,8]. In some cases, acoustic impedance alone may fail or not be enough to quantify reservoir rock properties such as lithology and pore fluid, for a detailed understanding of the reservoir. An additional parameterization related to the rock physics must therefore be utilized to fully characterize the reservoir. Elastic impedance may provide the additional parameterization for increasing the quality of the reservoir characterization in such cases. This is essentially the case with the present study.

Using a linearized version of the Zeoppritz equations, [3] derived a generalization of acoustic impedance for variable angles of incidence. This is known as elastic impedance (EI), and provides the framework to calibrate and invert high-angle seismic without reference to near offsets (angles). Elastic impedance (EI) as a function of P-wave angle of incidence, θ, is given by:

$$\text{EI}(\theta) = V_p^{(1+\tan^2\theta)}\, V_s^{-8k\sin^2\theta}\, \rho^{(1-4k\sin^2\theta)} \tag{1}$$

where V_p, V_s, ρ and θ are P-wave velocity, S-wave velocity, bulk density and P-wave angle of incidence, respectively, and k is a factor that is assumed to be constant and usually set to be equal to the average value of $(V_s/V_p)^2$ over the log interval of interest. One problem associated with elastic impedance is that it has strange dimensions (units) and the values do not scale correctly for different angles [9] as a result of raising velocity and density terms to increasing powers; the dimensions (units) vary with angle of incidence. To remove the dimensionality as a function of P-wave angle of incidence and provide elastic impedance with the same dimensionality, [9] introduced the normalization constants V_{p0}, V_{s0} and ρ_0, and normalized the elastic impedance (Equation 1) using:

$$\text{EI}(\theta) = V_{p_0}\rho_0\left[\left(\frac{V_p}{V_{p_0}}\right)^{(1+\tan^2\theta)} * \left(\frac{V_s}{V_{s_0}}\right)^{-8k\sin^2\theta} * \left(\frac{\rho}{\rho_0}\right)^{-4k\sin^2\theta}\right] \qquad (2)$$

In the present study, the model-based inversion methodology was utilized to invert the near angle stack for acoustic impedance. The implementation is based on the generalized linear inversion (GLI), and is well documented [10,5]. The method was successful in rock property prediction in three of four reservoirs in the well studied; the method identified the zones and tops of three of four reservoirs, but failed to successfully delineate the top of the fourth reservoir, which is the main reservoir in the well. Elastic impedance inversion targeted at the fourth reservoir not only revealed the reservoir, it clearly showed the reservoir top and its lateral extent, including other potential hydrocarbon exploration zones. This paper focuses on the post stack acoustic and elastic impedance inversion results and highlights their differences in the main reservoir.

1.1. Location and Geology

The study area is located in the Niger Delta offshore, tens of kilometers south of Port Harcourt (Figure 1).
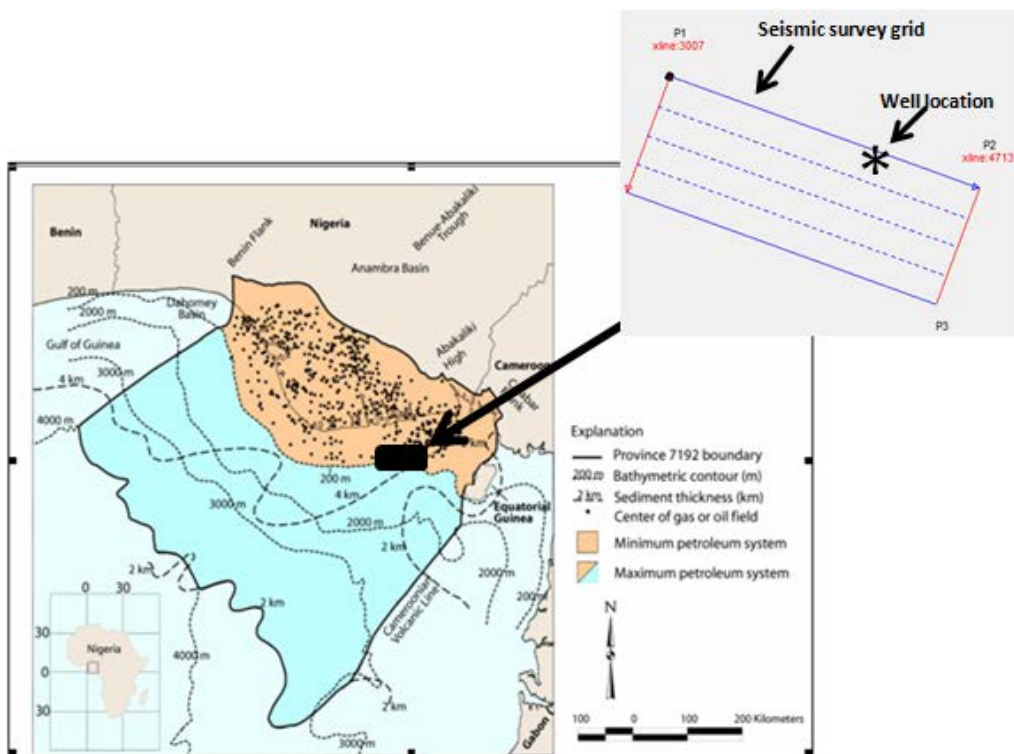

Figure 1: An Index Map of Nigeria and Cameroon. Map of the Niger Delta Showing Province Outline Maximum Petroleum System (After [11])

The Niger Delta is a prolific hydrocarbon province with a regressive succession of Tertiary age siliclastic sediments which are attributed to three lithostratigraphic formations, namely Akata, Agbada and Benin Formations. The Akata Formation is the basil unit of the Tertiary Niger Delta complex, and is made up

predominantly of massive and monotonous medium to hard, dark grey marine shales, with flora fossils in its upper part. The Agbada Formation overlies the Akata Formation, and is made up of alternating sequence of marine and fluvial sands and shales. This Formation ranges from Eocene in the North to Pliocene in the South and Recent at the delta surface, and represents the delta front, distributary channels and delta plain. The Benin Formation contains massive, highly porous continental sandstones and gravels with few shale interbeds. The Niger Delta province contains only one identified petroleum system, known as the Tertiary Niger Delta [12,13,14,15,16], and comprises the Akata shales and marine shales at the base of the Agbada Formation. Most of the hydrocarbon accumulations are in the sandstones of the Agbada Formation, where they are trapped in rollover anticlines fronting growth faults in channels and barrier sandstone bodies.

2. Materials and Methods

2.1. Materials

The data for the present study consist of well logs comprising measured GR, density, compressional and shear sonic logs acquired in a well in XYZ field, offshore Niger Delta, and $5^0 – 18^0$ (near-angle) and $30^0 – 42^0$ (far-angle) 3D PSTM stacks covering an area of 43.05 km^2. Figure 2 shows the measured GR, density, compressional and shear sonic logs, and acoustic and elastic impedance logs transformed from the original density, compressional and shear sonic logs.
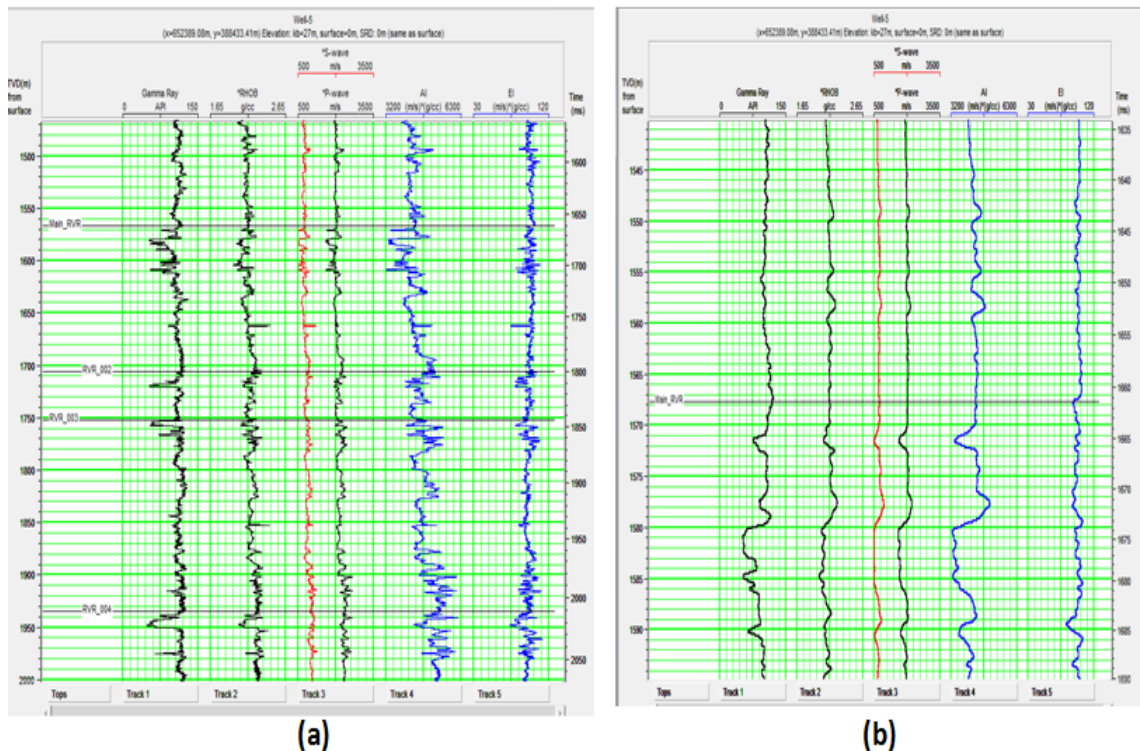

Figure 2: Well log data showing (a) measured GR log (Track 1); Bulk density log (Track 2); P- and S-wave sonic (Track 3); derived AI log (Track 4); derived EI log (Track 5). (b) zoomed display of log data.

2.2. Checkshot Correction, Well-to-seismic Correlation, Backgroud Model Building and Inversion

The first step in the inversion workflow was checkshot correction of the P-wave sonic log to match the two-way travel time of the seismic. Next, the well data were tied to the seismic to obtain a correction for the P-wave sonic at the well location. Wavelets were extracted from the seismic and well data to generate synthetic seismograms for this purpose. Seismic data are band-limited and do not contain low frequencies. Low frequency information is very critical in quantitatively predicting porosity, fluid content and other reservoir properties [17]. The lack of low frequencies prevents inverted impedance traces from having the basic impedances or velocity structure, critical to making a geological interpretation. This brings difficulty in reservoir prediction based on seismic inversion. Well logs however, are broadband, and contain low to very high frequency information of the order of kHz. Therefore in this study, well logs were used to provide the low impedance information missing from the seismic data.

Two background impedance models were initially created at the well location, and using the standard procedure of interpolation and extrapolation, the models were extended laterally to other parts of the survey guided by interpreted horizons. Four horizons were interpreted for this study, each picked to correspond to the top of each reservoir. Time map of the horizon picked at the main reservoir is shown in Figure 3. The first model created was an acoustic impedance model, generated from the density and corrected P-wave sonic logs. This was used to invert the near angle stack. The near angle stack has relative amplitudes similar to those at zero offset, but the summed seismic data have the advantage of improved signal-to-noise ratio compared to the zero offset data alone [5].
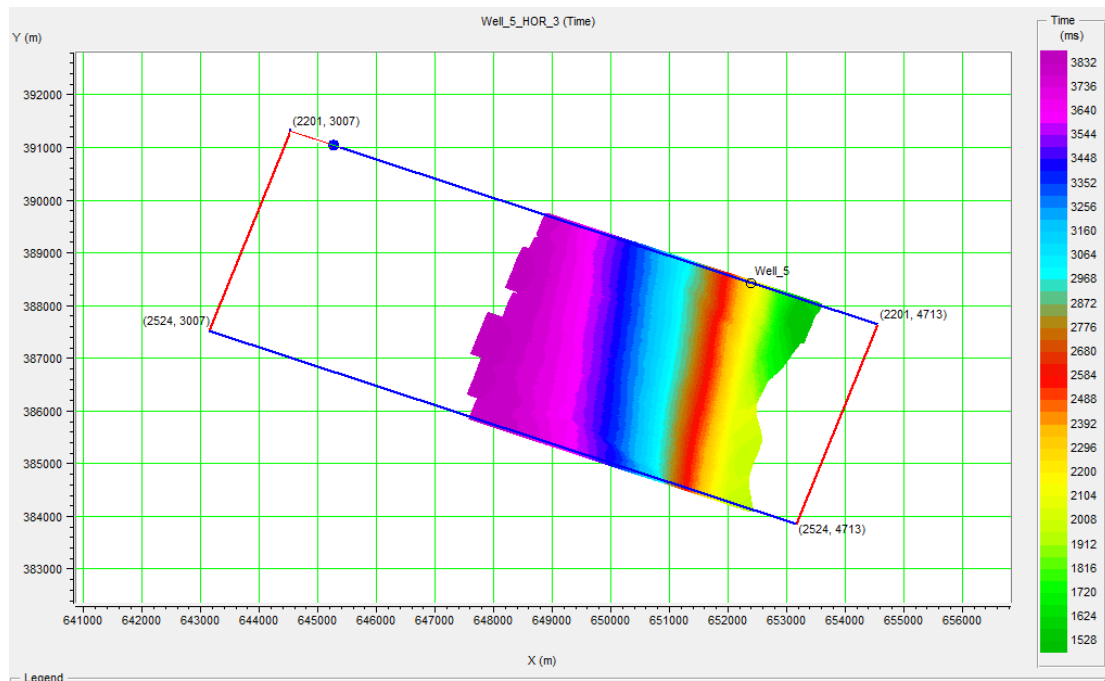

Figure 3: Time map of horizon at main reservoir top.

The second, an elastic impedance model, was generated from elastic impedance log created from the density,

shear sonic and corrected compressional sonic logs. The elastic impedance log was derived at 36^0 using Equation (1) with a constant $\dfrac{Vs}{Vp}$ ratio set to 0.55; this angle corresponds to the incidence angle for the far angle stack. This model was used to invert the far angle stack for elastic impedance. During each inversion procedure, a high-cut filter was applied at 8 Hz and 15 dB/Oct slope to the computed impedance log to retain the low frequencies not present in the seismic data in order to provide the background trend for the inversion. The model-based inversion algorithm was utilized to invert the individual volume, and ten recursive iterations of the initial model was performed in each case at a processing sample interval of 3 ms to generate the final optimized impedance volume.

3. Results and Discussion

Figure 4 shows the low frequency acoustic and elastic impedance models around the well location with inserted P-wave velocity log. Colour variations in the models depict changes in impedance corresponding to the individual model. Acoustic impedance varies from 10,552 to 20,854 ft/s*g/cc and elastic impedance varies from 245 to 358 ft/s*g/cc, indicating that colour variation is less in the elastic model than in the acoustic model.
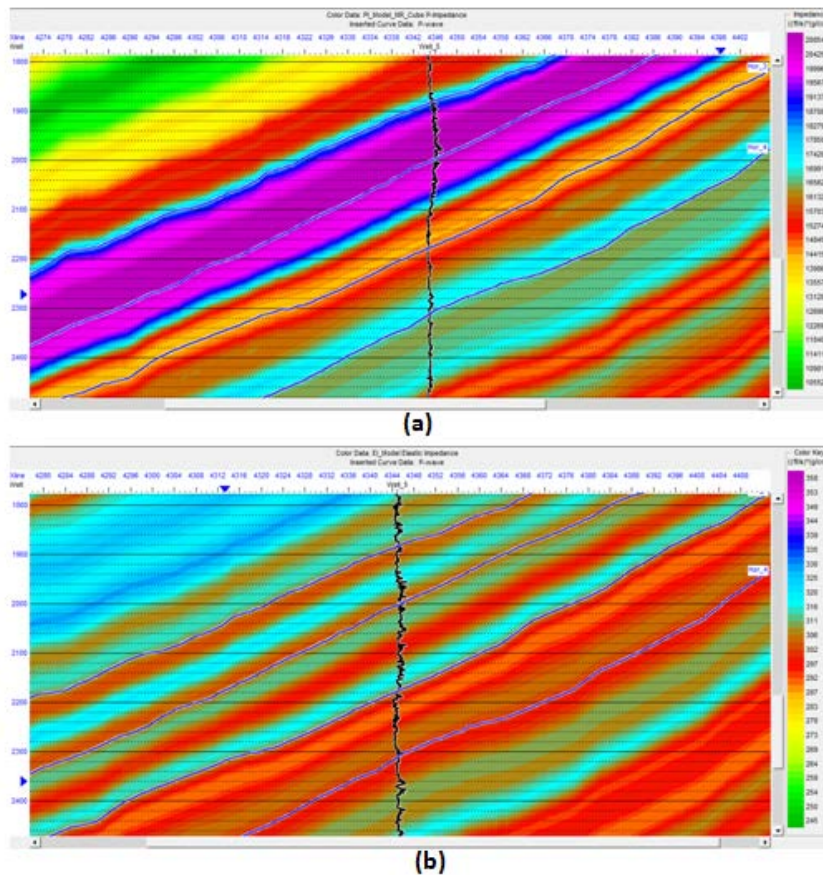

Figure 4: Low frequency background impedance models (a) acoustic impedance model generated from near volume (b) elastic impedance model generated from far volume.

Figure 5 shows the model-based analysis results of the acoustic and elastic impedance inversions at the well location. The correlation coefficient and percentage difference between predicted data and real seismic traces were 99% and 7.3% for the acoustic impedance model, and 99% and 12.5% for the elastic impedance model, respectively. The inverted acoustic and elastic impedance volumes around the well location are shown in Figure 6 and Figure 7, respectively. In comparison,
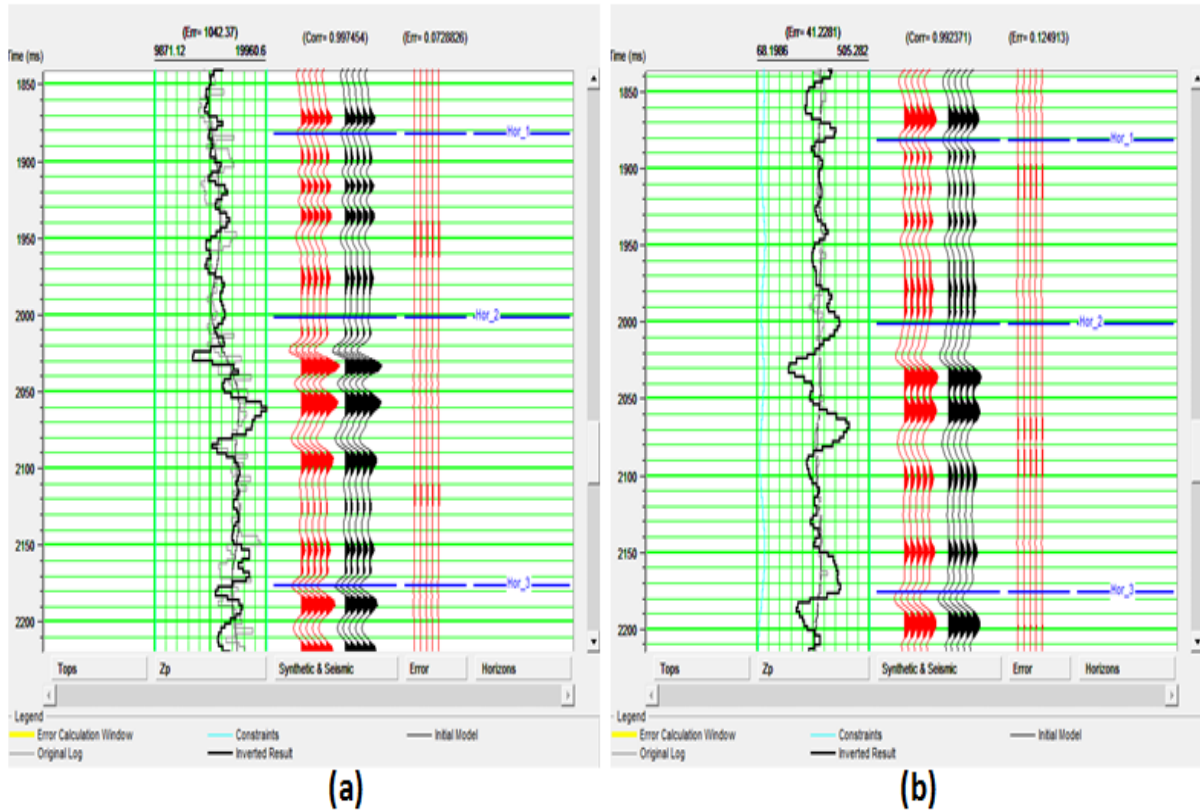

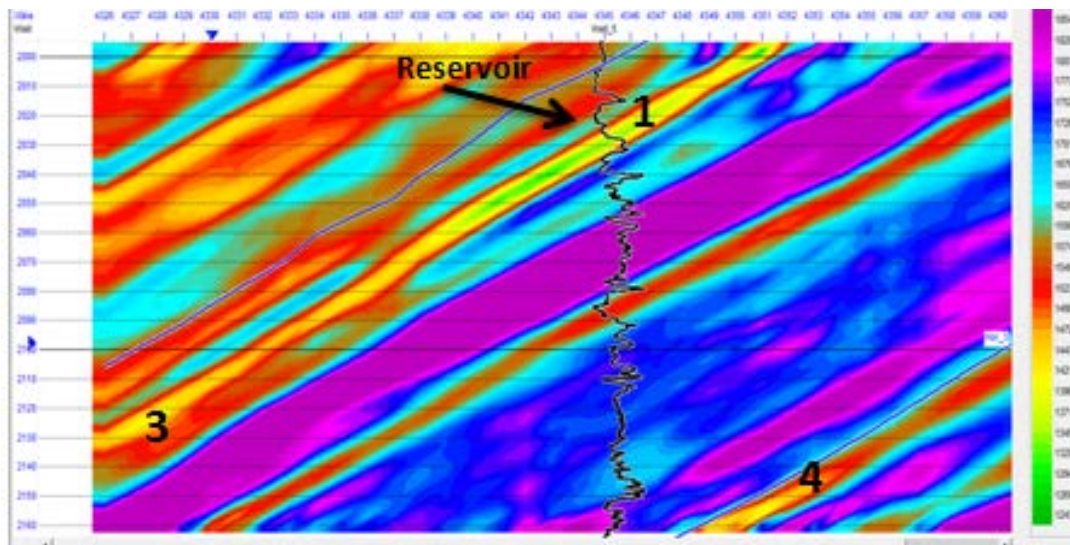**Figure 5:** Inversion analysis result at well location (a) acoustic impedance (b) elastic impedance

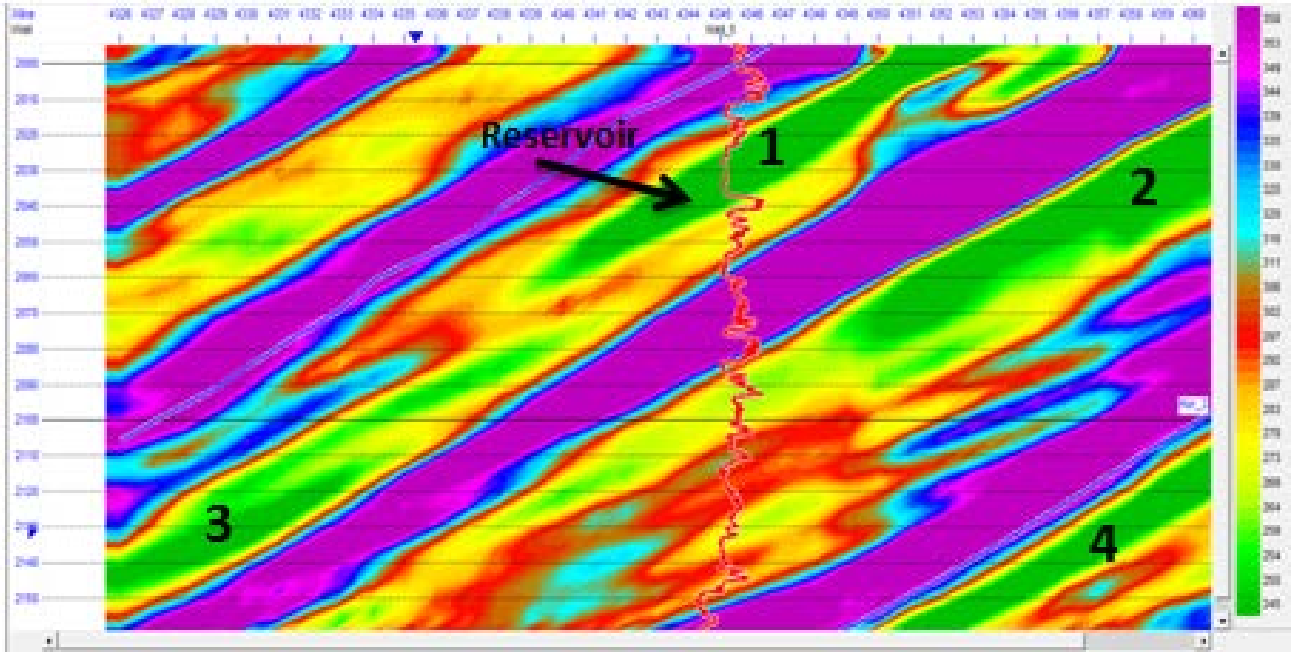**Figure 6:** Inverted acoustic impedance volume.

Figure 7: Inverted elastic impedance volume.

In comparison to the inverted acoustic impedance volume, the inverted elastic volume clearly shows the main reservoir (marked 1), as well as other low impedance anomalies away from well control (2, 3 and 4), which are not conspicuous in the acoustic impedance volume. The low impedance zones could be recognized in their own right as zones for potential low density hydrocarbon production. The tops and extents of the low impedance zones are clearly visible in the elastic impedance volume. High impedance shales transiting into the low impedance sandstone layers can be seen in the elastic impedance volume. Another feature seen in the elastic impedance volume is the extent of the low impedance anomalies. The shale lithologies extend spatially in larger areas than sands. The results show geologically consistent impedance values along the depositional dips in the impedance section.

One question that needs to be answered, however, is: why has the elastic impedance results inverted at 36^0 angle of incidence shown far more reliable and detailed results than the acoustic impedance volume inverted from the near angle stack, especially at the target main reservoir (indicated as 1 in Figures 6 and 7)? A possible explanation for this is shown in Figure 2b. The acoustic impedance (AI) log transformed from the density and P-wave sonic logs is nearly constant through the top reservoir transition. Expectedly, it would be difficult to easily determine the top reservoir from the inverted acoustic impedance section alone without additional rock physics-related parameterization. The 36^0 angle of incidence elastic impedance log derived from density, compressional and shear sonic logs shows a reasonable difference in values across the reservoir top; the values are reasonably lower transiting into the reservoir from its top than in the shale overlying the low impedance sands, implying that the reservoir top might be easily recognizable on the elastic impedance volume. The acoustic impedance volume, however, provides a better interpretation tool for detailed reservoir study in comparison to the input seismic volume (Figure 8).
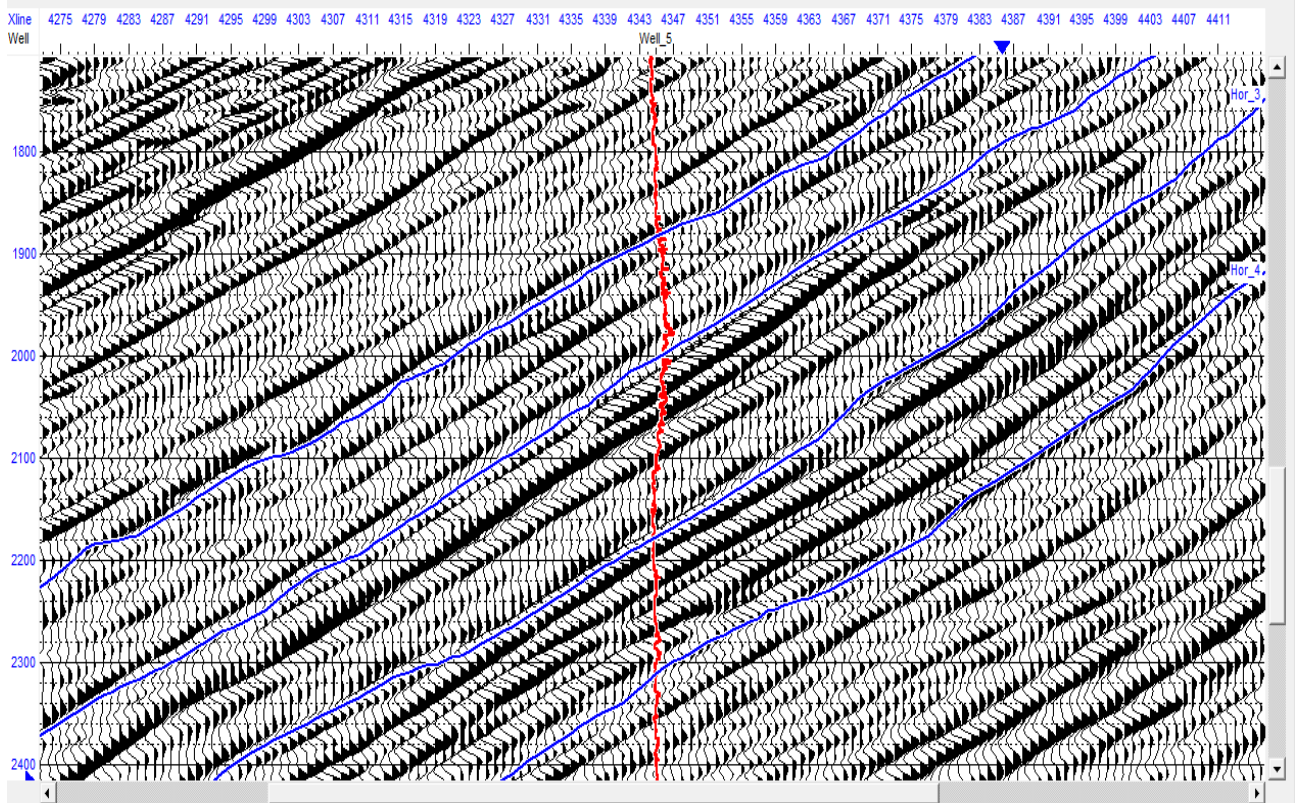
Figure 8: Near angle 3D PSTM stack input for inversion with inserted P-wave velocity log.

4. Conclusion

A near and far angle 3D PSTM stack was inverted for acoustic and elastic impedance respectively, in a bid to compare the inversion results and highlight differences at the main reservoir in the well studied. Both inversions were constrained by low frequency inputs from well logs. The elastic impedance results show more reliable and detailed results than the inverted acoustic impedance. The acoustic impedance log derived from the density and corrected P-wave sonic log is nearly constant and does not show any variation across the top reservoir transition; this may have accounted for the inability of the inversion to successfully locate the reservoir and delineate its top. The computed elastic impedance log shows reasonable reduction in values across the reservoir top hence, the elastic impedance inversion successfully located the reservoir and identified its top and lateral extent at and away from the wellbore, including other potential hydrocarbon prospective zones. A key element of this study is that post stack impedance inversion provides a tool for better understanding and characterization of reservoir, giving a more accurate result which can lead to a reduction in risking the successful development of field and well placement. The results can be integrated with additional rock physics information in the area to further improve quality of the results, especially in areas far away from well control.

References

[1] J. Pendrel, Seismic inversion – a critical tool in reservoir characterization, Scandinavian Oil-Gas Magazine, no. 5/6, pp. 19-22, 2006.

[2] K. Duffaut, T. Alsos, M. Landro, H. Rogno, and N. Al-Najjar, Shear wave elastic impedance, The Leading Edge, 1222-1229, 2000.

[3] P. Connolly, Elastic impedance: The Leading Edge, v. 18, p. 438–452, 1999.

[4] S. Inichinbia, P.O. Sule, A.L. Ahmed and H. Hamza, AVO inversion and lateral prediction of reservoir properties of Amangi hydrocarbon field of the Niger Delta area of Nigeria, IOSR Journal of Applied Geology and Geophysics, 2(2), pp. 8-17, 2014.

[5] L. Keumsuk, Y. Dong-Geun, M. George, H. Namsoon, and H.L. Gwang, A two-dimensional post stack seismic inversion for acoustic impedance of gas hydrate bearing deep-water sediments within thecontinental slope of the Ulleung Basin, East Sea, Korea, Terr. Atmos. Ocean. Sci., Vol. 24, No. 3, 295-310, 2013.

[6] P.F. Anderson, Comparing post-stack AVO inversion to pre-stack inversion for estimating rock properties, Frontiers+Innovation, CSPG, CSEG, CWLS Convention, Canada, 2009.

[7] C. Wagner, A. Gonzalez, V. Argawal, A. Koesoemadinata, D. Ng, S. Trares, N. Biles, and K. Fisger, Quantitative application of post stack acoustic impedance inversion to subsalt reservoir development, The   Leading Edge, 528-537, 2012.

[8] P.F. Anderson and L.R. Lines, A comparison of inversion techniques for estimating Vp/Vs from 3D seismic data, CREWES Research Report, Vol. 20, 2008.

[9] D.N. Whitcombe, Elastic impedance normalization, Geophysics, v. 67, no. 1, p. 60-62, 2002.

[10] D.A. Cooke and W.A. Schneider, Generalized inversion of reflection seismic data, Geophysics, 48, 665- 676, 1983.

[11] Petroconsultants, Petroleum exploration and production database: Houston, 1996.

[12] B.H. Russell, K. Hedlin, F.J. Hilterman and L.R. Lines, Fluid-property discrimination with AVO: A Biot-Gassmann perspective, Geophysics, 68, 2003, 29-39.

[13] J.M. Orife and A.A. Avbovbo, Stratigraphic and unconformity traps in the Nige Delta: AAPG Bulletine. 66(2): 1982, 251-262.

[14] C.M. Ekweozor. and E.M. Daukoru, Niger Delta depobelt portion of the Akata-Agbada petroleum

system, AAPG Memoir 60, 1994, 599-604.

[15] H. Kulke, Regional Geology of the world, part 2: Africa, America, Austrialia.Antarctica: Berlin Gebrulder borntraeger, Kulke Ed.: 1995 143-172.

[16] T.J.A. Reijers, S.W. Peter and C.S. Nwajide, The Niger Delta Basin: In Reijers,T.J.A. Ed., Selected Chapters on Geology; SPDC, Warri, 1996, 103-118.

[17] Z. Zou, L. Ling, Y.J. Wang, J. Gao and X.Y. Xi, Low-frequency impedance modeling based on well logs and seismic attributes, 75th EAGE Conference and Exhibition, London, UK, 2013.